Angiotensin receptor blockers, but not angiotensin-converting enzyme inhibitors, inhibit abnormal bone changes in spondyloarthritis

Jin Sun Choi
Chungnam National University Hospital
Ji-Young Kim
Chungnam National University Hospital
Min-Joo Ahn
Chungnam National University Hospital
Hanbit Jang
Chungnam National University Hospital
Seungtaek Song
Chungnam National University Hospital
Sungsin Jo
Hanyang University Institute for Rheumatology Research, Hanyang University
Sung Hoon Choi
Hanyang University Hospital
Ye-Soo Park
Hanyang University College of Medicine
Tae-Hwan Kim
Hanyang University Hospital for Rheumatic Diseases
Seung Cheol Shim (shimsc@cnuh.co.kr)
Chungnam National University Hospital

Research Article

Keywords: Angiotensin II receptor blocker, Angiotensin-converting enzyme inhibitor, Osteoclast, Osteoblast, Renin-angiotensin system, Spondyloarthritis

Posted Date: January 19th, 2023

DOI: https://doi.org/10.21203/rs.3.rs-2482526/v1

Abstract

Background

Spondyloarthritis (SpA) is a chronic inflammatory disease that results in bone ankylosis. The tissue renin-angiotensin system (RAS), updated with new components, is an emerging phenomenon possibly implicated in SpA-associated bone changes. Therefore, we sought to determine the mechanism underlying this relationship.

Methods

Sakaguchi (SKG) mice injected with curdlan (SKGc), animal models for SpA, were treated with the RAS modulators, angiotensin II receptor blockers (ARBs) or angiotensin-converting enzyme inhibitors (ACEis). Disease activity was assessed using clinical scores and computed tomography scans. Mouse primary bone marrow monocytes (BMMs), osteoblast (OB) progenitor cells, peripheral blood monocytes (PBMCs), and bone-derived cells (BdCs) from patients with radiographic axial SpA (r-axSpA) were used to investigate the role of RAS in SpA pathogenesis.

Results

The expression of RAS components was significantly high in SKGc mouse joints, wherein ARBs significantly reduced erosion and systemic bone loss, whereas ACEis did not. Osteoclast (OC) differentiation from primary BMMs, mediated by TRAF6, was inhibited by ARBs but promoted by ACEis; the modulators also exerted opposite effects on OB differentiation. Expression of RAS molecules was higher in PBMCs and BdCs of patients with r-axSpA than in control participants. ARBs inhibited OB differentiation in the BdCs of patients with r-axSpA, whereas ACEi did not. Neither ARBs nor ACEis affected OB differentiation in the control participants.

Conclusions

In SpA, a condition characterized by RAS overexpression, ARBs, but not ACEis, inhibited OC and OB differentiation and bone progression. These findings must be considered when treating patients with SpA using RAS modulators.

Background

Spondyloarthritis (SpA), a chronic inflammatory disease, is characterized by a unique bone phenotype resulting from simultaneous increase in bone formation and resorption [1, 2], culminating in skeletal damage and functional impairment [3, 4]. Although long-term use of tumor necrosis factor blockers [5, 6]

may reduce radiographic progression, particularly in the early phase of the disease, novel therapies targeting bone changes in SpA are required.

The renin-angiotensin system (RAS) is classically viewed as an endocrine system that regulates hemodynamic equilibrium, circulating volume, and electrolyte balance [7]. Angiotensinogen, secreted by the liver, is cleaved by renin, an enzyme produced in the kidneys, to form angiotensin (Ang I). Ang I is then cleaved by angiotensin-converting enzyme (ACE) to form Ang II, an effector hormone that acts through its traditional receptor, Ang II receptor 1 (AT1R) [8]. RAS modulators, such as ACE inhibitors (ACEis) and angiotensin receptor blockers (ARBs), are widely used to treat hypertension and heart and kidney diseases [9–14].

Challenging this traditional view of RAS, new components, such as ACE2 and Ang 1–7, have recently been identified [15]. ACE2, an enzyme that converts Ang II to Ang 1–7 [16], has been extensively studied in recent years owing to its role as an entry point for coronavirus disease [17, 18]. Ang 1–7 is also generated by neprilysin (neutral endopeptidase, NEP) from Ang I [19].

Along with the classical pathway, components of the RAS are expressed and exert specific local effects in multiple tissues, a phenomenon referred to as tissue RAS [7, 20]. RAS components, particularly the major effector protein Ang II and its receptors, are expressed in the local milieu of bones and regulate bone metabolism [21]. Animal studies have demonstrated that tissue RAS plays a key role in postmenopausal [22], age-related [23], and glucocorticoid-induced [24] osteoporosis. Additionally, RAS components expressed by T cells, natural killer cells, macrophages, and dendritic cells are involved in immune activation [25]. Tissue RAS is also involved in chronic inflammatory disorders, such systemic lupus erythematosus [26] and rheumatoid arthritis (RA) [27]. A recent study on an animal model of RA showed that Ang II exacerbates bone erosion [28]. However, the role of the newer components of RAS, effect of RAS modulators on bone cells, and role of RAS in SpA are yet to be explored.

Therefore, in this study, we used an in vivo model of SpA, an in vitro culture system of osteoclasts (OCs) and osteoblasts (OBs), and human samples to investigate the potential role of RAS in abnormal bone changes induced by SpA, the different effects of each RAS modulator, and the mechanisms via which RAS modulators affect bone cell differentiation.

Materials And Methods

Experimental mouse model and clinical scoring

Female SKG mice were purchased from CLEA Japan, Inc. (Tokyo, Japan) and were maintained under specific pathogen-free conditions. Eleven-week-old female SKG mice were intraperitoneally injected with 3 mg curdlan (Wako, Osaka, Japan; SKGc). The experimental animals were divided into four groups: negative control (n = 5 mice), vehicle (saline, n = 15), losartan treatment (n = 12; SK Chemicals, South Korea), and enalapril treatment (n = 10; Chong Kun Dang Pharmaceutical Corp., South Korea). Losartan, an AT1R blocker, and enalapril, an ACEi (10 mg/kg each), were administered to the treatment groups for

five days a week, from day 0 to 56. The clinical signs of the mice were monitored twice per week and scored by two independent observers. The severity of arthritis was assessed via the clinical arthritis score and myeloperoxidase (MPO) activity obtained using an in vivo imaging system (IVIS) with a XenoLight RediJect inflammation probe (PerkinElmer, Waltham, MA, USA). Clinical arthritis scores were evaluated on a scale of 0 to 4 for each limb (0, no swelling; 1, slight swelling and erythema; 2, moderate swelling and erythema; 3, severe swelling and erythema; and 4, maximal inflammation with joint rigidity). Thus, the maximum possible score for each mouse was 16 [29].

Analysis of bony changes in the ankle joints of SKGc mice

Bone deformities in the ankle joints of the mice were analyzed using a Quantum FX micro-computed tomography (CT) (PerkinElmer, Waltham, MA, USA). The micro-CT settings used were as follows: energy/intensity of 90 kVp, electric current of 160 μA, sampling time of 3 min, and field of view of 5 mm. Three-dimensional views were constructed using the 3D viewer imaging software program (PerkinElmer, USA).

Erosions were defined as clear juxta-articular breaks in the cortical shell. Osteophytes were defined as bony protrusions of the juxta-articular cortical shell. Erosions and osteophytes were evaluated on the following scale: 0, no surface changes; 1, surface changes on <25% of the surface; 2, surface changes on >25% and <50% of the surface; and 3, surface changes on >50% of the surface [30].

Patient samples and human primary bone-derived cells (BdCs)

All studies involving human materials were performed in compliance with the Helsinki Declaration and approved by the Ethics Committee of Chungnam University Hospital and Hanyang University Hospital; written informed consent was obtained from all subjects (IRB-2015-03-020, IRB-2014-05-001, and IRB-2014-05-002). Human blood samples were collected from 6 patients with r-axSpA who met the Assessment of SpondyloArthritis International Society classification criteria and 8 healthy controls. PBMCs were separated from whole blood via Ficoll-Paque density gradient centrifugation (GE Healthcare, USA). Human bone tissues were obtained during surgery from the facet joints of 7 patients with r-axSpA and 7 patients with non-inflammatory spinal disease as controls. Primary bone-derived cells (BdCs) derived from vertebral bone tissue obtained during spinal surgery in AS patients were provided by Dr. Tae -Hwan Kim (Department of Rheumatology, Hanyang University Hospital for Rheumatic Diseases, Seoul, South Korea). Human primary BdCs were cultured as reported previously [31]. In primary BdCs, matrix maturation during osteoblast differentiation was assessed via alkaline phosphatase (ALP; Sigma-Aldrich, St. Louis, MO, USA, 85L2) staining. The matrix mineralization of osteoblast differentiation was assessed using ARS (Sigma-Aldrich, A5533), hydroxyapatite HA (Lonza, PA-1503), and Von Kossa (Sigma-Aldrich, S7179) staining.

Reagents

The following reagents were used in the in vitro experiments: losartan potassium (ARB; Sigma-Aldrich, SML3269), captopril (ACEi; Sigma-Aldrich, C4042), angiotensin II (Sigma-Aldrich, A6402), angiotensin 1-7 (R & D Systems, Minneapolis, MN, 1562), MLN-4760 (ACE2i; Sigma-Aldrich, 530616), sacubitrilat (NEPi; MedChem Express, Shanghai, China, HY-17620), bradykinin (R & D Systems, 3004), bradykinin receptor inhibitor (R & D Systems, HOE 140), and Mas receptor inhibitor (R & D Systems, A779).

OC differentiation from mouse primary bone marrow-derived cells

Mouse BMMs, isolated by flushing the marrow space of the femur and tibia in 5-week-old mice, were incubated overnight on culture dishes in α-minimal essential medium (MEM) (Gibco Laboratories, Grand Island, NY, USA) containing 10% fetal bovine serum (FBS) (Gibco Laboratories) and antibiotics (100 units/mL penicillin G and 100 μg/mL streptomycin; Gibco Laboratories) at 37 °C in a humidified atmosphere containing 5% CO_2 and 95% air. After discarding adherent cells, the floating cells were further incubated with mouse macrophage colony stimulating factor (M-CSF) (30 ng/mL; Peprotech, USA) on Petri dishes. The BMMs became adherent after 3 days in culture, and the cells were differentiated into OCs after treatment with RANKL (50 ng/mL; Peprotech) and M-CSF (30 ng/mL) for 5 days.

OB differentiation from mouse primary calvarial cells

ICR mice were purchased from DBL Co., Ltd. (South Korea). Murine calvarial cells were obtained from the calvaria of 1–3-day-old ICR mice and incubated for 15 min in α-MEM containing 0.1% collagenase (Gibco Laboratories) and 0.2% dispase (Gibco Laboratories) with shaking. The supernatant was collected and centrifuged for 5 min at 1,600 rpm. This step was repeated five times. Primary mouse calvarial cells were maintained in α-MEM with 10% FBS and antibiotics (100 units/mL penicillin G and 100 μg/mL streptomycin) at 37 °C in a humidified atmosphere containing 5% CO_2 and 95% air, and were differentiated into OBs following treatment with ascorbic acid (50 μg/mL; Sigma-Aldrich) and 10 mM β-glycerophosphate (Sigma-Aldrich) for 7–21 days.

Tartrate-resistant acid phosphatase activity assay

After the BMMs were differentiated into OCs for 5 days, the cells were fixed with 4% formaldehyde for 15 min. Then, the cells were washed and stained for tartrate-resistant acid phosphatase (TRAP) using a TRAP staining kit (TaKaRa Biotechnology, Otsu, Japan), according to the manufacturer's instructions. TRAP-positive multinucleated cells (MNCs) containing three or more nuclei were counted as mature OCs under a light microscope. All experiments were performed in triplicate with independent samples.

ALP staining and activity assay and matrix mineralization assay

After the cells were seeded in 24-well culture plates and differentiated for 7 and 21 days, they were fixed with 4% formaldehyde for 15 min. Then, the cells were washed, and ALP activity was determined using an ALP staining kit (TaKaRa Biotechnology) and an ALP yellow (pNPP) liquid substrate system (Sigma-Aldrich). To assess the matrix mineralization phase, alizarin red staining (ARS; Sigma-Aldrich) was used

to determine calcium deposition. For ARS quantification, the stained wells were treated with 10% cetylpyridinium chloride (Sigma -Aldrich). The supernatant was transferred to a 96-well plate and the absorbance was read at an excitation wavelength of 540 mM using an enzyme-linked immunosorbent assay (ELISA) plate reader.

RNA isolation and reverse-transcription quantitative polymerase chain reaction (RT-qPCR) analysis

Total RNA was extracted using the TRIzol reagent (Molecular Research Center, Genbiotech SRL, Argentina), according to the manufacturer's protocol. Reverse transcription was performed using ReverTra Ace qPCR RT master mix with a gDNA remover kit (Toyobo, Osaka, Japan), following the manufacturer's instructions. Amplification of 1 µL cDNA was performed using the iQ^{TM} SYBR Green Supermix (Bio-Rad Laboratories, Hercules, CA, USA). RT-qPCR was performed using a CFX96 real-time PCR detection system (Bio-Rad Laboratories). The expression of mouse and human target genes was normalized to that of the *18S rRNA* and *HuPo*, which were used as housekeeping genes. The normalized expression values were averaged, and the average fold changes were calculated. The detailed primer sequences are provided in Table S1. Three independent experiments were performed to determine the mRNA levels.

ELISA

The levels of angiotensin 1-7 and bradykinin in the supernatant collected from captopril (ACEi)-stimulated cells were determined using an ELISA kit (R & D Systems), according to the manufacturer's protocol (NBP2-69079; Novus Biologicals, USA).

Western blotting

Protein extracts were isolated from each group of cells using RIPA lysis buffer (Sigma-Aldrich) containing 1 mM complete protease inhibitor cocktail (Sigma-Aldrich). Total protein was separated using 10% sodium dodecyl sulfate-polyacrylamide gel electrophoresis (SDS-PAGE), transferred to a nitrocellulose membrane, blocked in 5% bovine serum albumin (BSA), probed with appropriate primary antibodies against the target proteins (anti-TRAF6, sc-8409, 1:200, Santa Cruz Biotechnology, Inc.; anti-β-Actin, A1978, 1:5000, Sigma–Aldrich) overnight at 4 °C, and then incubated with horseradish peroxidase-conjugated secondary antibodies (goat anti-mouse IgG H&L, ab6708, 1:10000, Abcam; goat anti-rabbit IgG H&L, ab6721, 1:10000, Abcam) at room temperature for 1 h. Protein bands were detected using a chemiluminescence reagent (Thermo Fisher Scientific).

Cell counting kit-8 (CCK-8) assay for cell viability

Cell viability was determined using the (CCK-8) assay. Briefly, the cells were plated in 96-well plates at the density of 1×10^4 cells/well. After drug treatment, the cells were incubated for 4 h with CCK-8 reagent (Dojindo Molecular Technologies, Inc., Shanghai, China), following which absorbance was measured at 450 nm using a microplate reader.

Statistical analysis

Statistical analysis was performed using the GraphPad Prism software. The Mann-Whitney *U* test was performed for two-group comparisons, and data with $p < 0.05$ were considered statistically significant. All results are presented as the mean ± standard deviation (SD).

Results

Expression of RAS components was upregulated in the joints of SKGc mice and the PBMCs and BdCs of r-axSpA patients

To determine the expression of RAS components in the arthritic joints of an animal model of SpA, SKG mice were injected with curdlan to generate SKGc mice (Fig. 1a). The expression of RAS components in the joints of SKGc mice was assessed using RT-qPCR and western blotting. The expression levels of AGT, ACE, and AT1R were significantly higher in the joints of SKGc mice than in those of wild type (WT) or SKG mice (p = 0.025, 0.034, and0.014, respectively; Fig. 1b). Western blotting revealed that the protein levels of AGT, ACE, and AT1R in the ankle joints of SKGc mice were higher than those in WT or SKG mice (Fig. S1).

We also compared the expression of RAS molecules between patients with r-axSpA and control participants. First, we identified the RAS molecules in the PBMCs of patients with r-axSpA and control participants. The expression levels of AGT, ACE, AT1R, AT2R, and NEP were significantly higher (p = 0.003, 0.0037, 0.005, 0.025, and 0.0306, respectively) in the PBMCs of patients with r-axSpA than in those of the control participants (Fig. 1c). Next, we compared the expression of RAS molecules in BdCs between patients with r-axSpA and control participants. The expression levels of all RAS molecules, except for AT2R, were significantly higher (p = 0.027, 0.003, 0.05, and 0.032, respectively) in r-axSpA patients than in control participants (Fig. 1d).

ARBs, but not ACEis, inhibited bone erosion and systemic bone loss in SKGc mice

RAS affects the development of inflammation [32]. Hence, we investigated whether RAS modulators, such as ARBs and ACEis, influence the development of arthritis in SKGc mice. First, we monitored the severity of paw swelling in each limb and compared the clinical arthritis scores among SKGc groups treated with the vehicle, ARB, or ACEi (SKGc-saline, SKGc-ARB, or SKGc-ACEi, respectively). No significant differences were observed between the groups (Fig. 2a). Next, we measured MPO activity using IVIS; however, we did not find any differences between the groups (Fig. 2b).

Additionally, joint tissues were stained with hematoxylin and eosin to determine the degree of inflammatory cell infiltration in the ankle joints of SKGc mice. Compared to that in WT mice, SKGc-saline mice showed increased inflammatory cell infiltration in the joints. There was no difference in the degree of inflammatory cell infiltration among SKGc-saline, SKGc-ARB, and SKGc-ACEi mice, which is consistent with the results on the clinical arthritis score and MPO activity (Fig. S2). Thus, RAS modulators did not significantly affect the severity of arthritis in SKGc mice.

Next, we performed CT of arthritic joints to assess the effect of RAS modulation on the development of erosion and abnormal bone formation. The CT erosion score was significantly lower in SKGc-ARB mice (p = 0.033) and higher in SKGc-ACEi mice than in SKGc-saline mice (p = 0.898) (Fig 2c and d, left). CT bone formation scores decreased in SKGc-ARB mice (p = 0.515) and increased in SKGc-ACEi mice (p = 0.516) compared to that in SKGc-saline mice (Fig. 2c and d, right).

Furthermore, bone CT was used to investigate the effect of RAS modulation on bone remodeling. Bone mineral density (BMD) was significantly higher in the SKGc-ARB group (p = 0.011) and lower in the SKGc-ACEi group (p = 0.462) than in the SKGc-saline group (Fig. 2e and f). Differences were not observed in the BMD measurement of mice in the WT-saline, WT-ARB, and WT-ACEi groups treated with each RAS modulator (to determine whether these drugs affected BMD in a non-inflammatory environment) (Fig. S3a and b).

Next, we measured the expression levels of bone cell-related molecules in the joints of SKGc mice. The expression levels of OC differentiation markers, such as TRAP, NFATc, and cathepsin K, were significantly lower in SKGc-ARB mice than in SKGc-saline mice (p = 0.006, 0.006, and 0.006, respectively); however, differences were not observed between SKGc-ACEi and SKGc-saline mice (p = 0.522, 0.670, and 0.394, respectively) (Fig. 2g). Similarly, the expression of OB differentiation markers such as BMP2, RUNX2, and RANKL was significantly lower in SKGc-ARB mice (p = 0.006, 0.006, and 0.006, respectively) but higher in SKGc-ACEi mice than in SKGc-saline mice (p = 0.286, 0.088, and 0.394, respectively) (Fig. 2h).

ARB and ACEi showed opposite effects on osteoclast differentiation from mouse primary bone marrow macrophages

To verify the direct role of RAS in bone cells, we applied RAS modulators in bone cell culture systems. First, we administered ARB or ACEi to the BMMs of mice. TRAP staining revealed that OC differentiation was significantly inhibited by ARB (p = 0.006), but significantly promoted by ACEi (p = 0.004), compared to that in the controls (Fig. 3a). ACEi increased the numbers of TRAP-positive multinucleated OCs and OCs with more than 30 nuclei per cell (p = 0.002; Fig. S4). Differences in cell viability were not observed among the groups in the CCK8 assay (Fig. 3b). RT-qPCR analysis revealed that ARB significantly lowered (p = 0.006, 0.028, 0.009, 0.009, and 0.009, respectively) whereas ACEi increased (p = 0.006, 0.028, 0.009, 0.021, and 0.009, respectively) the expression of OC differentiation markers, such as TRAP, NFATc, cathepsin K, DC-STAMP, and OC-STAMP compared to that in the controls (Fig. 3c).

To investigate the signals acting upstream of the above-mentioned factors, we measured the expression level of TRAF6 in RAW 264.7 cells treated with saline, ARB, or ACEi; ARB inhibited the expression of TRAF6, but ACEi did not (Fig. 3d). To further investigate the mechanism underlying the inhibition, cells were treated with MG132, a proteasome inhibitor, which restored TRAF6 expression (Fig. 3e), suggesting that the effect of RAS modulators on OCs was mediated via TRAF6 ubiquitination, resulting in degradation by the proteasome.

Ang 1-7 facilitated osteoclast differentiation from mouse primary bone marrow macrophages

The conflicting effects of ARB and ACEi led us to hypothesize that contrary to previous reports [22, 33, 34], Ang 1-7, rather than Ang II, might play a dominant role in OC differentiation. To verify this, we first confirmed that Ang 1-7 levels increased significantly (p = 0.021) after the treatment of OC progenitors with ACEi (Fig. 4a).

To examine the effect of Ang 1-7 on OC differentiation, we treated the cells with saline, Ang 1-7, or Ang II. TRAP staining revealed that Ang 1-7 enhanced OC differentiation (p = 0.004; Fig. 4b) and the expression of target molecules, including TRAP, NFATc, cathepsin K, DC-STAMP, OC-STAMP, OSCAR, and Blimp1 (p = 0.020, 0.018, 0.017, 0.019, 0.017, 0.019, and 0.019, respectively), to an extent similar to that observed with Ang II (Fig. 4c). Both Ang II and Ang 1-7 increased the expression of TRAF6, contrary to that observed with ARB (Fig. 4D).

We hypothesized that the increase in OC differentiation after treatment with Ang II was caused by Ang 1-7 derived from Ang II, and not by Ang II itself. Therefore, we simultaneously administered Ang II and ACE2i to OC progenitor cells to inhibit the conversion. This diminished the promoting effect of Ang II on OC differentiation to a level similar to that of the control group (Fig. 4e). Furthermore, Ang 1-7 levels decreased when ACE2i was used in combination with Ang II compared to Ang II alone (Fig. S5). Additionally, the NEP inhibitor (NEPi), administered with Ang I, completely blocked OC differentiation (p = 0.002; Fig. 4f), implying that NEP might be a critical enzyme involved in Ang 1-7 production, at least in the bone milieu. OC differentiation was inhibited by NEPi (p = 0.004) without changes in cell viability (Fig. S6a and b), and the mRNA expression of target molecules, including TRAP, NFATc, cathepsin K, DC-STAMP, and OC-STAMP,decreased after NEPi treatment (p = 0.008, 0.008, 0.008, 0.008, and 0.009, respectively; Fig. S6c). These results, combined with the finding that ACEi promoted OC differentiation, suggested that Ang 1-7, rather than Ang II, plays a major role in OC differentiation.

Furthermore, a Mas receptor (MasR) inhibitor (MasRi) was used to assess OC differentiation, as MasR is the major receptor of Ang 1-7. MasRi treatment significantly increased OC differentiation (p = 0.009; Fig. 4g). Additionally, to determine whether Ang 1-7 acted on the AT1 receptor, we treated OC progenitor cells simultaneously with Ang 1-7 and ARB, which suppressed the Ang 1-7-induced promotion of OC differentiation (Fig. 4b and c). To verify this further, ACEi and ARB were simultaneously administered to the cells. We observed that OC differentiation was inhibited without changes in cell viability (Fig. S7a and b), and expression of the OC differentiation marker decreased (Fig. S7c). Thus, the Ang 1-7/AT1 axis is the major pathway involved in OC differentiation.

ARB and ACEi exerted opposite effects on osteoblast differentiation from mouse primary osteoblast progenitor cells

To examine the effect of ARB and ACEi on OB differentiation, mouse OB progenitor cells were treated with RAS modulators in an in vitro culture system. Intracellular ALP activity assay and alizarin red staining (ARS) were performed to assess OB differentiation and mineralization, respectively. Intracellular ALP activity in OBs was suppressed by ARB (p = 0.021) but promoted by ACEi (p = 0.11), suggesting that ARB and ACEi exerted opposite effects on OB differentiation despite the lack of statistical significance (Fig.

5a). ARS analysis revealed that ARB significantly inhibited (p = 0.021), whereas ACEi promoted (p = 0.043) mineralization (Fig. 5b) without changes in cell viability (Fig. 5c). Consistent with these findings, we observed that compared to the vehicle, ARB significantly decreased the expression of bone formation markers, including BMP2, RUNX2, RANKL, and osteocalcin, in OBs (p = 0.021, 0.020, 0.021, and 0.021, respectively), whereas ACEi significantly increased their expression levels (p = 0.043, 0.248, 0.149, and 0.021, respectively) (Fig. 5d). Experiments using the human SaOS2 cell line produced similar results (Fig. S8a and b).

Additionally, Ang 1-7 increased OB differentiation and mineralization to a degree similar to that of Ang II (Fig. 5e and f). When cells were co-stimulated by ARB and ACEi, OB differentiation and mineralization were inhibited without changes in cell viability (Fig. S9a–c).

ARB inhibited osteoblast differentiation from BdCs of r-axSpA patients

We investigated whether RAS modulators affect the differentiation of OBs obtained from patients with r-axSpA. ARB and ACEi were administered to the BdCs of biologic-naïve r-axSpA patients and control participants. ALP, ARS, and Von Kossa staining revealed that ARB significantly inhibited OB differentiation and mineralization in biologic-naïve r-axSpA patients (p = 0.0058, 0.042, 0.003, and 0.0144, respectively), whereas ACEi did not (Fig 6a and b, right panels). Significant changes were not observed in the OBs of the control participants treated with ARB or ACEi (Fig. 6a and b, left panels). Additionally, HA staining and bright field imaging showed that ARB inhibited the mineralization of OBs in the r-axSpA patients, but not in the control participants (Fig. 6c).

Discussion

Our findings indicated that RAS is involved in the differentiation of OBs and OCs, and that RAS components are overexpressed in SpA. To the best of our knowledge, this is the first study to demonstrate the role of RAS in the pathogenesis of SpA. As RAS expression is upregulated in the PBMCs and bone cells of patients with r-axSpA, its modulation may effectively inhibit abnormal bone changes in patients with SpA. The effect of RAS modulators, however, depends on their type.

There are several plausible mechanisms via which systemic RAS may affect bone changes. RAS regulates the immune system [32], which can indirectly affect bone remodeling, and interacts with calcium-regulating hormones [35, 36]. However, we did not find any significant differences in clinical arthritis scores, MPO activity, and inflammatory cell infiltration among the control, ARB-treated, or ACEi-treated groups. Thus, the bone changes modulated by ARB and ACEi in SpA were not due to their effect on inflammation. Therefore, we performed in vitro studies to verify the direct effects of RAS on bone cells. Surprisingly, ARB and ACEi exerted different effects in animal models and in vitro culture systems, which is supported by the results of other studies on RAS modulators and osteoporosis. For example, treatment with the ARB, olmesartan, significantly reduced the decline in femoral neck BMD in bedridden elderly female hypertension patients with disuse syndrome [37]. Kwok et al. showed that ACEi use correlated

with a small but significant increase in bone loss at the hip, whereas ARB use did not [38]. Another study conducted in Taiwan reported increase in osteoporotic fractures with ACEi use, but not with ARB [39].

However, whether RAS modulators affect osteoporosis development in patients receiving these medications remains unclear [40], as double-blind placebo-controlled prospective studies have not yet been conducted. Generally, individuals receiving hypertensive medication are older and at the risk of developing osteoporosis. In our study, ARB significantly inhibited systemic bone loss in SKGc mice, which can be explained by the high expression of RAS molecules presumed to cause bone loss. However, RAS modulators may not exert a significant effect on BMD in the general population in which expression of RAS molecules is low, as ARB did not affect BMD in WT mice. Corroborating this claim, a recent study demonstrated that Ang II enhances bone erosion in a mouse model of RA, but does not induce systemic bone loss in WT mice. As r-axSpA patients showed higher expression of RAS components than control participants, ARB could inhibit osteoporosis in patients with r-axSpA. The mechanisms underlying the increase in the expression of RAS components warrant further clarification.

We found that ARB inhibited abnormal bone formation, increased BMD, and decreased OB and OC differentiation, whereas ACEi did not affect abnormal bone formation or BMD but increased OB and OC differentiation. Although Ang II is the main effector in bone metabolism [22, 33, 34], our findings suggest that Ang 1–7 might be another important factor, as ACEi increased both OC and OB differentiation. ACEi increased the concentration of Ang 1–7 by inhibiting the conversion of Ang I to Ang II, thereby allowing the conversion of Ang 1 to Ang 1–7, and simultaneously inhibiting the degradation of Ang 1–7 to inactive Ang 1–5. Our in vitro studies with Ang 1–7 and enzyme inhibitors, including ACE2i and NEPi, indicated that Ang 1–7 might be an active mediator of bone metabolism. Nozato et al. reported that Ang 1–7 significantly increased bone volume in WT and *Ace2*-knockout mice [41], which supports our hypothesis. Recently, Sha et al. reported that Ang 1–7 increased the formation of calcific nodules and ALP activity in OB cells, as well as bone mineralization, and decreased osteoclast differentiation via MasR in the presence of high levels of glucose [42]. These findings are consistent with our observation regarding OBs, but not OCs. This discrepancy may be attributed to the hyperglycemic conditions in the previous study. We also postulate that Ang 1–7 may act on both MasR and AT1R and exert different effects depending on the receptor it binds to. The effect of Ang II on osteoclastogenesis has been reported to be exerted via Ang 1–7 conversion. However, further studies are required to decipher the precise roles of Ang II and Ang 1–7 in bone cells.

Moreover, our in vitro observations imply that in addition to RANKL signaling, RAS signaling is integral to the activation of TRAF6, a molecule acting upstream in osteoclastogenesis. ACEi did not increase TRAF6 expression, but increased NFATc expression at the mRNA level, suggesting that additional downstream signals may be activated by ACEi.

Nevertheless, this study had some limitations. First, although Ang 1–7 acts on AT1R [43], we did not directly investigate whether Ang 1–7 binds to AT1R in OBs and OCs. As Ang II has higher affinity for AT1R, the interaction between Ang II and Ang 1–7 may differentially affect bone cell differentiation.

Further studies are required to provide compelling evidence regarding this. Second, factors other than Ang 1–7 may explain the differences observed between ARB and ACEi. For example, in our study, bradykinin and Ang 1–7 promoted OC differentiation (p = 0.002 and 0.002, respectively; Fig. S10a). However, this effect was not inhibited by the bradykinin inhibitor (Fig. S11a). Additionally, bradykinin levels did not differ significantly between the ACEi-treated and control groups (Fig. S12a), suggesting that ACEi exerts minimal effect on bradykinin degradation in the bone milieu. In contrast, Ang 1–7 levels increased significantly in the ACEi-treated group, indicating that Ang 1–7 was a more likely candidate than bradykinin in promoting OC differentiation. Third, the precise mechanisms via which Ang 1–7 enhances OB differentiation remain unclear. Furthermore, the sample size used in this study was relatively small, because of which the statistical power required to detect small but significant differences may be lacking. Therefore, future studies with larger sample sizes are warranted.

This study has several important clinical implications. This is possibly the first study to suggest that RAS and its modulation may affect bone phenotype in SpA. The RAS modulator, ARB, significantly reduced bone erosion and increased BMD in an animal model of SpA, implying that ARBs may be better than ACEis for treating hypertension in patients with SpA. Our in vitro results also suggest that Ang 1–7 may play an important role in the differentiation of bone cells.

Conclusion

Tissue RAS plays an important role in OC and OB differentiation, ARB and ACEi exert different effects on abnormal bone changes in SpA (Fig. 7), and Ang 1–7 may be a major effector of bone cell differentiation. Additionally, RAS may act as a therapeutic target in SpA. Further clinical studies on the effects of RAS modulators in patients with SpA are required.

Abbreviations

ACE
Angiotensin-converting enzyme
ACEi
Angiotensin-converting enzyme inhibitor
ALP
Alkaline phosphatase
AGT
Angiotensinogen
Ang II
Angiotensin II
Ang 1–7
Angiotensin 1–7
ARB
Angiotensin II receptor blocker

ARS
Alizarin red
AT1R
Angiotensin II type 1 receptor
AT2R
Angiotensin II type 2 receptor
BdC
Bone-derived cell
BF
Bright field
BMD
Bone mineral density
BMM
Bone marrow macrophage
BMP2
Bone morphogenetic protein 2
CT
Computed tomography
DC-STAMP
Dendritic cell-specific transmembrane protein
HA
Hydroxyapatite
MasRi
Mas receptor inhibitor
MNC
Multi-nuclear cells
MPO
Myeloperoxidase
NEPi
neprilysin inhibitor
NFATc
Nuclear factor of activated T cell
OB
Osteoblast
OC
Osteoclast
OC-STAMP
Osteoclast stimulatory transmembrane protein
PBMC
Peripheral blood mononuclear Cell

RAS
Renin-angiotensin system
r-axSpA
radiographic axial spondyloarthritis
Runx2
Runt-related transcription factor 2
SKG
Sakaguchi
SKGc
curdlan-induced Sakaguchi
SpA
Spondyloarthritis
TRAP
Tartrate-resistant acid phosphatase

Declarations

Ethics approval and consent to participate

This study was approved by the Institutional Review Boards of Chungnam University Hospital (IRB-2015-03-020), Hanyang University Hospital (IRB-2014-05-001), and Hanyang University Guri Hospital (IRB-2014-05-002). It was conducted in accordance with the principles of the Declaration of Helsinki. Written informed consent was obtained from all participants. All mice experimental procedures were assessed and approved by the Institutional Animal Care and Use Committee of the Chungnam National University Hospital (CNUH-019-A0025) and were conducted in accordance with the Laboratory Animals Welfare Act and Guide for the Care and Use of Laboratory Animals.

Consent for publication

Not applicable.

Availability of data and materials

The datasets generated and analyzed during this study will be available on reasonable request to the corresponding author.

Competing interests

None of the authors declare any conflict of interest.

Funding

This work was supported by the Basic Science Research Program through the National Research Foundation of Korea (NRF) funded by the Ministry of Education (grant numbers, NRF-2016R1A6A3A11934500, NRF-2019R1I1A1A01060116, and NRF-2019R1I1A3A01060016). It was also supported by the Chungnam National University Hospital Research Fund (grant numbers, 2016-CF-003).

Author contribution

JSC designed all experiments and analyzed the data. JSC, J-YK, and SCS contributed to the conception and design. JSC, J-YK, and SJ performed both in vivo and in vitro experiments. SHC and Y-SP provided human facet joint samples. SJ and T-HK provided human osteoprogenitor cells. JSC, M-JA, HJ, SS, and SCS analyzed the data. All authors read and approved the final manuscript.

Acknowledgments

We thank Professor Tae-Hwan Kim (Hanyang University Hospital for Rheumatic Diseases) for providing the human osteoprogenitor cells derived from facet joints in this study.

References

1. Sieper J, Poddubnyy D. Axial spondyloarthritis. Lancet. 2017;390:73-84.
2. Braun J, Sieper J. Ankylosing spondylitis. Lancet. 2007;369:1379-90.
3. Sharif K, Watad A, Tiosano S, Yavne Y, Blokh Kerpel A, Comaneshter D, et al. The link between COPD and ankylosing spondylitis: a population based study. Eur J Int Med. 2018;53:62-5.
4. Benucci M, Damiani A, Bandinelli F, Grossi V, Infantino M, Manfredi M, et al. Ankylosing spondylitis treatment after first anti-TNF drug failure. Isr Med Assoc J. 2018;20:119-22.
5. Sepriano A, Ramiro S, Wichuk S, Chiowchanwisawakit P, Paschke J, van der Heijde D, et al. Tumor necrosis factor inhibitors reduce spinal radiographic progression in patients with radiographic axial spondyloarthritis: a longitudinal analysis from the Alberta Prospective Cohort. Arthritis Rheumatol. 2021;73:1211-9.
6. Karmacharya P, Duarte-Garcia A, Dubreuil M, Murad MH, Shahukhal R, Shrestha P, et al. Effect of therapy on radiographic progression in axial spondyloarthritis: A systematic review and meta-analysis. Arthritis Rheumatol. 2020;72:733-49.
7. Bader M. Tissue renin-angiotensin-aldosterone systems: Targets for pharmacological therapy. Ann. Rev. Pharmacol. Toxicol. 2010;50:439-65.
8. Sparks MA, Crowley SD, Gurley SB, Mirotsou M, Coffman TM. Classical renin-angiotensin system in kidney physiology. Compr. Physiol. 2014;4:1201-28.
9. Yusuf S, Sleight P, Pogue J, Bosch J, Davies R, Dagenais G. Effects of an angiotensin-converting-enzyme inhibitor, ramipril, on cardiovascular events in high-risk patients. New Engl J Med. 2000;342:145-53.

10. Yusuf S, Pitt B, Davis CE, Hood WB, Jr., Cohn JN. Effect of enalapril on mortality and the development of heart failure in asymptomatic patients with reduced left ventricular ejection fractions. New Engl J Med.1992;327:685-91.
11. Lewis EJ, Hunsicker LG, Clarke WR, Berl T, Pohl MA, Lewis JB, et al. Renoprotective effect of the angiotensin-receptor antagonist irbesartan in patients with nephropathy due to type 2 diabetes. New Engl J Med. 2001;345:851-60.
12. Lewis EJ, Hunsicker LG, Bain RP, Rohde RD. The effect of angiotensin-converting-enzyme inhibition on diabetic nephropathy. The Collaborative Study Group. New Engl J Med. 1993;329:1456-62.
13. Dahlöf B. Left ventricular hypertrophy and angiotensin II antagonists. Am J Hypertens. 2001;14:174-82.
14. Brenner BM, Cooper ME, de Zeeuw D, Keane WF, Mitch WE, Parving HH, et al. Effects of losartan on renal and cardiovascular outcomes in patients with type 2 diabetes and nephropathy. New Engl J Med. 2001;345:861-9.
15. Santos RAS, Sampaio WO, Alzamora AC, Motta-Santos D, Alenina N, Bader M, et al. The ACE2/Angiotensin-(1-7)/MAS axis of the renin-angiotensin system: focus on angiotensin-(1-7). Physiol Rev. 2018;98:505-53.
16. Patel VB, Zhong JC, Grant MB, Oudit GY. Role of the ACE2/Angiotensin 1-7 axis of the renin-angiotensin system in heart failure. Circ Res. 2016;118:1313-26.
17. Scialo F, Daniele A, Amato F, Pastore L, Matera MG, Cazzola M, et al. ACE2: the major cell entry receptor for SARS-CoV-2. Lung. 2020;198:867-77.
18. Bourgonje AR, Abdulle AE, Timens W, Hillebrands JL, Navis GJ, Gordijn SJ, et al. Angiotensin-converting enzyme 2 (ACE2), SARS-CoV-2 and the pathophysiology of coronavirus disease 2019 (COVID-19). J Pathol. 2020;251:228-48.
19. Domenig O, Manzel A, Grobe N, Königshausen E, Kaltenecker CC, Kovarik JJ, et al. Neprilysin is a mediator of alternative renin-angiotensin-system activation in the murine and human kidney. Sci Rep. 2016;6:33678.
20. Lee MA, Böhm M, Paul M, Ganten D. Tissue renin-angiotensin systems. Their role in cardiovascular disease. Circulation. 1993;87(5 Suppl):Iv7-13.
21. Mo C, Ke J, Zhao D, Zhang B. Role of the renin-angiotensin-aldosterone system in bone metabolism. J Bone Miner Metab. 2020;38:772-9.
22. Shimizu H, Nakagami H, Osako MK, Hanayama R, Kunugiza Y, Kizawa T, et al. Angiotensin II accelerates osteoporosis by activating osteoclasts. FASEB J. 2008;22:2465-75.
23. Gu SS, Zhang Y, Li XL, Wu SY, Diao TY, Hai R, et al. Involvement of the skeletal renin-angiotensin system in age-related osteoporosis of ageing mice. Biosci Biotechnol Biochem. 2012;76:1367-71.
24. Yongtao Z, Kunzheng W, Jingjing Z, Hu S, Jianqiang K, Ruiyu L, et al. Glucocorticoids activate the local renin-angiotensin system in bone: possible mechanism for glucocorticoid-induced osteoporosis. Endocrine. 2014;47:598-608.

25. Jurewicz M, McDermott DH, Sechler JM, Tinckam K, Takakura A, Carpenter CB, et al. Human T and natural killer cells possess a functional renin-angiotensin system: further mechanisms of angiotensin II-induced inflammation. J Am Soc Nephrol. 2007;18:1093-102.
26. Teplitsky V, Shoenfeld Y, Tanay A. The renin-angiotensin system in lupus: physiology, genes and practice, in animals and humans. Lupus. 2006;15:319-25.
27. Chang Y, Wei W. Angiotensin II in inflammation, immunity and rheumatoid arthritis. Clin Exp Immunol. 2015;179:137-45.
28. Akagi T, Mukai T, Mito T, Kawahara K, Tsuji S, Fujita S, et al. Effect of angiotensin II on bone erosion and systemic bone loss in mice with tumor necrosis factor-mediated arthritis. Int J Mol Sci. 2020;21:4145.
29. Ruutu M, Thomas G, Steck R, Degli-Esposti MA, Zinkernagel MS, Alexander K, et al. β-glucan triggers spondylarthritis and Crohn's disease-like ileitis in SKG mice. Arthritis Rheum. 2012;64:2211-22.
30. Stach CM, Bäuerle M, Englbrecht M, Kronke G, Engelke K, Manger B, et al. Periarticular bone structure in rheumatoid arthritis patients and healthy individuals assessed by high-resolution computed tomography. Arthritis Rheum. 2010;62:330-9.
31. Jo S, Wang SE, Lee YL, Kang S, Lee B, Han J, et al. IL-17A induces osteoblast differentiation by activating JAK2/STAT3 in ankylosing spondylitis. Arthritis Res Ther. 2018;20:115.
32. Crowley SD, Rudemiller NP. Immunologic effects of the renin-angiotensin system. J Am Soc Nephrol. 2017;28:1350-61.
33. Tamargo J, Caballero R, Delpón E. The renin–angiotensin system and bone. Clin Rev Bone Miner Metab. 2015;13:125-48.
34. Hatton R, Stimpel M, Chambers TJ. Angiotensin II is generated from angiotensin I by bone cells and stimulates osteoclastic bone resorption in vitro. J Endocrinol. 1997;152:5-10.
35. Zheng MH, Li FX, Xu F, Lin X, Wang Y, Xu QS, et al. The interplay between the renin-angiotensin-aldosterone system and parathyroid hormone. Front Endocrinol. 2020;11:539.
36. Vaidya A, Brown JM, Williams JS. The renin-angiotensin-aldosterone system and calcium-regulatory hormones. J Hum Hypertens. 2015;29:515-21.
37. Aoki M, Kawahata H, Sotobayashi D, Yu H, Moriguchi A, Nakagami H, et al. Effect of angiotensin II receptor blocker, olmesartan, on turnover of bone metabolism in bedridden elderly hypertensive women with disuse syndrome. Geriatr Gerontol Int. 2015;15:1064-72.
38. Kwok T, Leung J, Zhang YF, Bauer D, Ensrud KE, Barrett-Connor E, et al. Does the use of ACE inhibitors or angiotensin receptor blockers affect bone loss in older men? Osteoporos Int. 2012;23:2159-67.
39. Butt DA, Mamdani M, Gomes T, Lix L, Lu H, Tu K. Risk of osteoporotic fractures with angiotensin II receptor blockersversus angiotensin-converting enzyme inhibitors in hypertensive community-dwelling elderly. J Bone Miner Res. 2014;29:2483-88.
40. Izzo JL, Jr., Weir MR. Angiotensin-converting enzyme inhibitors. J Clin Hypertens. 2011;13:667-75.

41. Nozato S, Yamamoto K, Takeshita H, Nozato Y, Imaizumi Y, Fujimoto T, et al. Angiotensin 1-7 alleviates aging-associated muscle weakness and bone loss, but is not associated with accelerated aging in ACE2-knockout mice. Clin Sci. 2019;133:2005-18.
42. Sha NN, Zhang JL, Poon CC, Li WX, Li Y, Wang YF, et al. Differential responses of bone to angiotensin II and angiotensin(1-7): beneficial effects of ANG(1-7) on bone with exposure to high glucose. Am J Physiol Endocrinol Metab. 2021;320:E55-70.
43. Nicklin SA. A novel mechanism of action for angiotensin-(1-7) via the angiotensin type 1 receptor. Hypertension. 2016;68:1342-3.

Figures

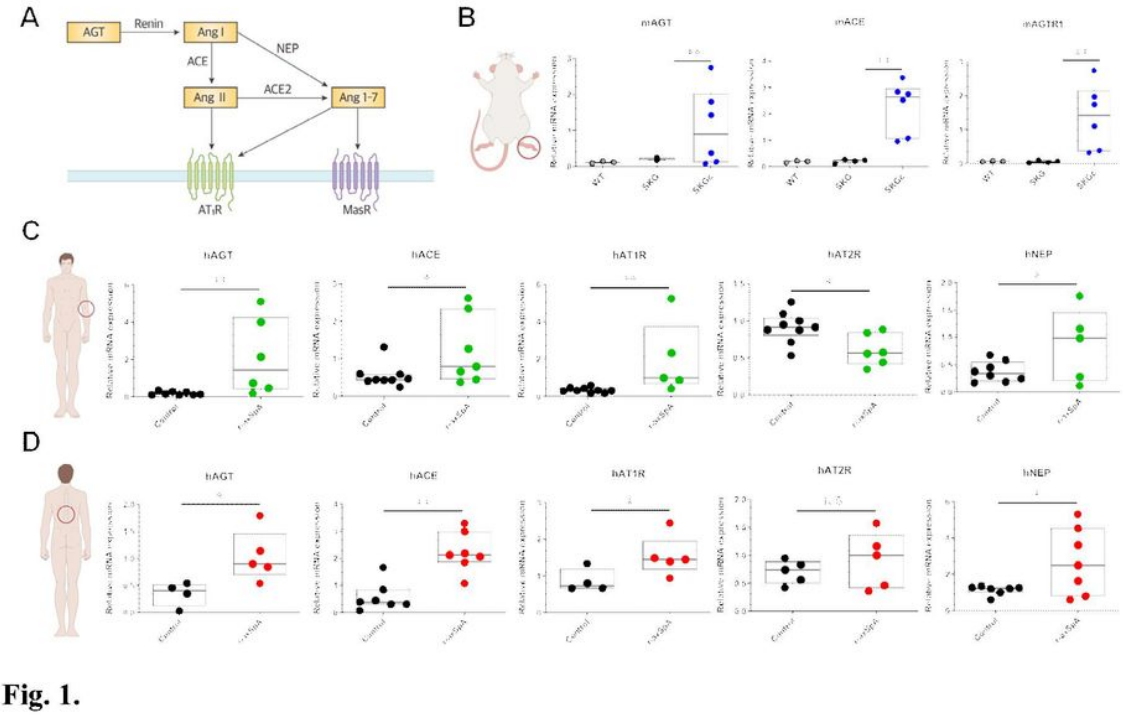

Fig. 1.

Figure 1

Expression levels of RAS components increased in SKGc mice and patients with r-axSpA. (a) Schematic representation of the renin-angiotensin system (RAS). (b-c) RT-qPCR analysis of RAS component-related gene expression in (b) ankle joint tissues of wild type (WT; n = 3), SKG (n = 3), and SKGc (n = 5) mice; (c) PBMCs of control (n = 8) and r-axSpA patients (n = 6); (d) bone-derived cells of control (n = 7) and r-axSpA patients (n = 7). ACE, angiotensin-converting enzyme; AGT, angiotensinogen; AT1/2R, angiotensin

II type 1/2 receptor; NEP, neutral endopeptidase; SKG, Sakaguchi; SKGc, curdlan-induced SKG; r-axSpA, radiographic axial spondyloarthritis; N.S., not significant. Values are presented as mean ± SD.; *$p < 0.05$, **$p < 0.01$ using Mann-Whitney U test.

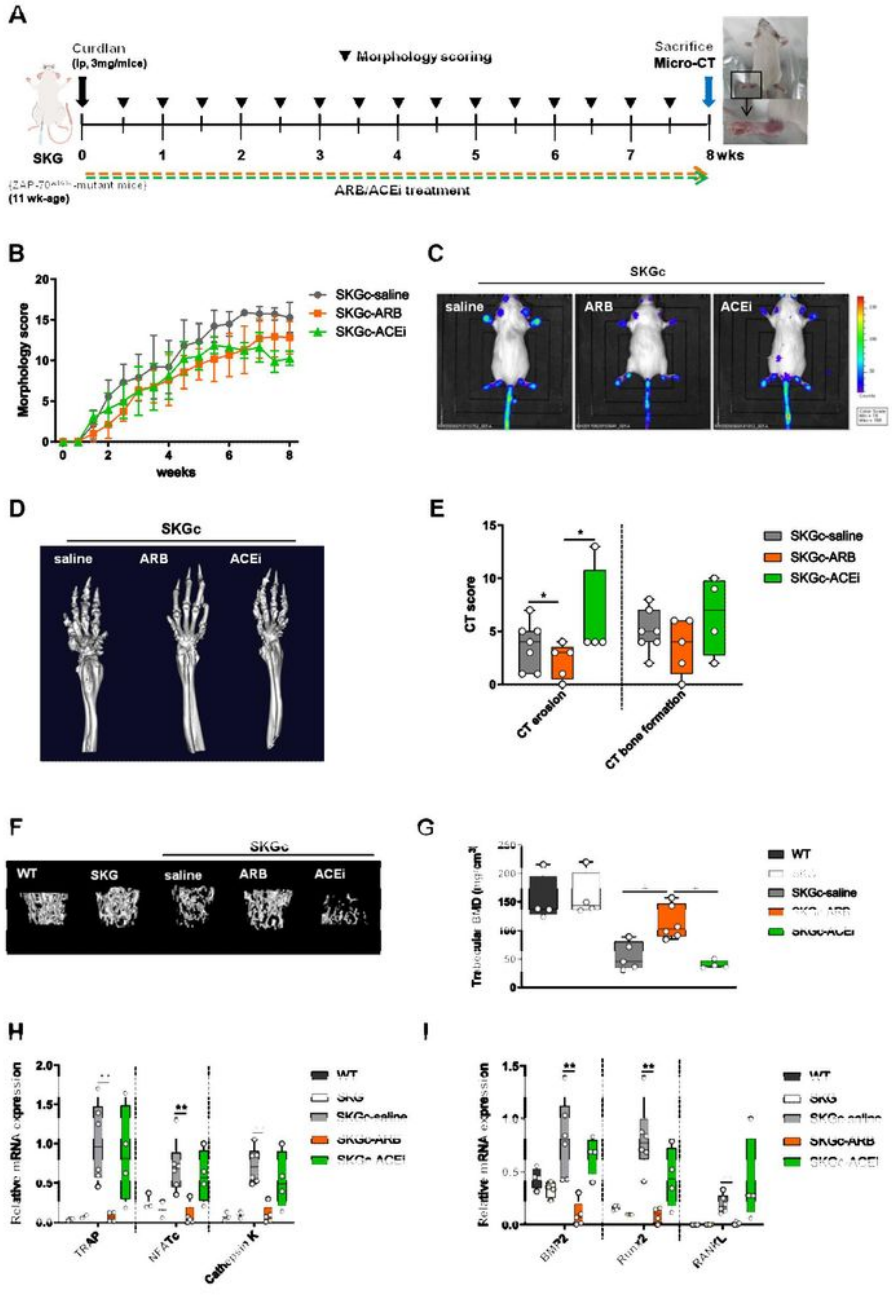

Fig. 2.

Figure 2

ARB and ACEi differentially affected bony changes, but did not affect clinical arthritis in SKGc mice. (a) Experimental design. Arthritis was induced in SKG mice by injecting 3 mg curdlan (SKGc), and samples were acquired at 8 weeks. (b-i) SKGc mice treated with saline, ARB (10 mg/kg losartan), or ACEi (10 mg/kg enalapril). (b) Morphology scoring. (c) MPO activity measured using IVIS. (d) Micro-CT images of ankle joints. (e) CT scoring of bone erosion and formation. (f) Micro-CT images of trabecular bones. (g) Measurement of BMD. mRNA expression of osteoclast (h) and osteoblast (i) differentiation markers in ankle joints (n = 5 for group). 18S RNA expression was used for normalization. ACEi, angiotensin-converting enzyme inhibitor; ARB, angiotensin II receptor blocker; SKG, Sakaguchi; SKGc, curdlan-induced SKG. Values are presented as mean ± SD.; *$p < 0.05$, **$p < 0.01$ using Mann-Whitney U test.

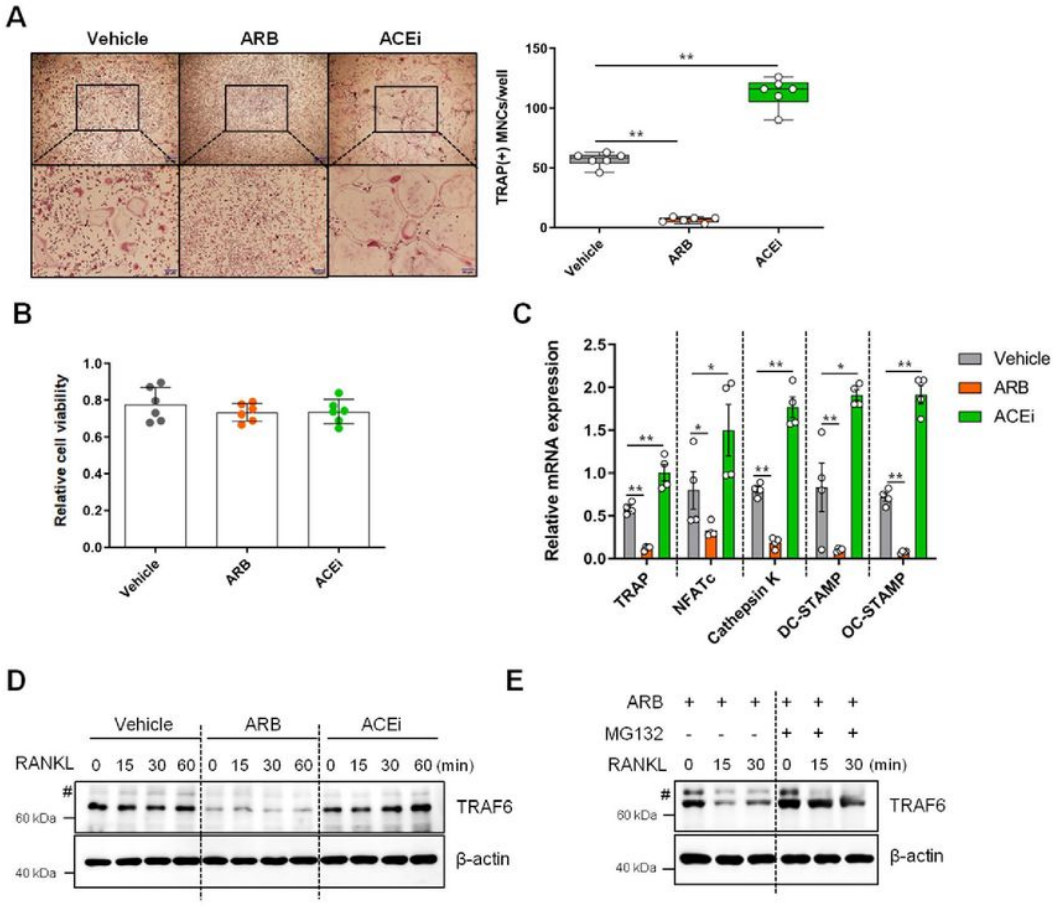

Fig. 3.

Figure 3

ARB inhibited and ACEi promoted osteoclast differentiation in mouse cells. (a-c) Mouse bone marrow monocytes were treated with ARB (1×10^{-5} M losartan) or ACEi (1×10^{-5} M captopril). (a) Representative TRAP staining images (left) and the number of TRAP-positive MNCs (>3 nuclei) per well (right). Scale bar = 50 μm. (b) CCK-8 assay. (c) RT-qPCR analysis. (d) Western blotting analysis of ARB- or ACEi-treated RAW 264.7 cells. (e) Western blotting analysis of ARB-treated RAW 264.7 cells with/without MG132 treatment. Hash symbol (#) indicates nonspecific bands. ACEi, angiotensin-converting enzyme inhibitor; ARB, angiotensin II receptor blocker; MNCs, multi-nuclear cells; TRAP, tartrate-resistant acid phosphatase. Values are presented as mean ± SD.; *$p < 0.05$, **$p < 0.01$ using Mann-Whitney *U* test.

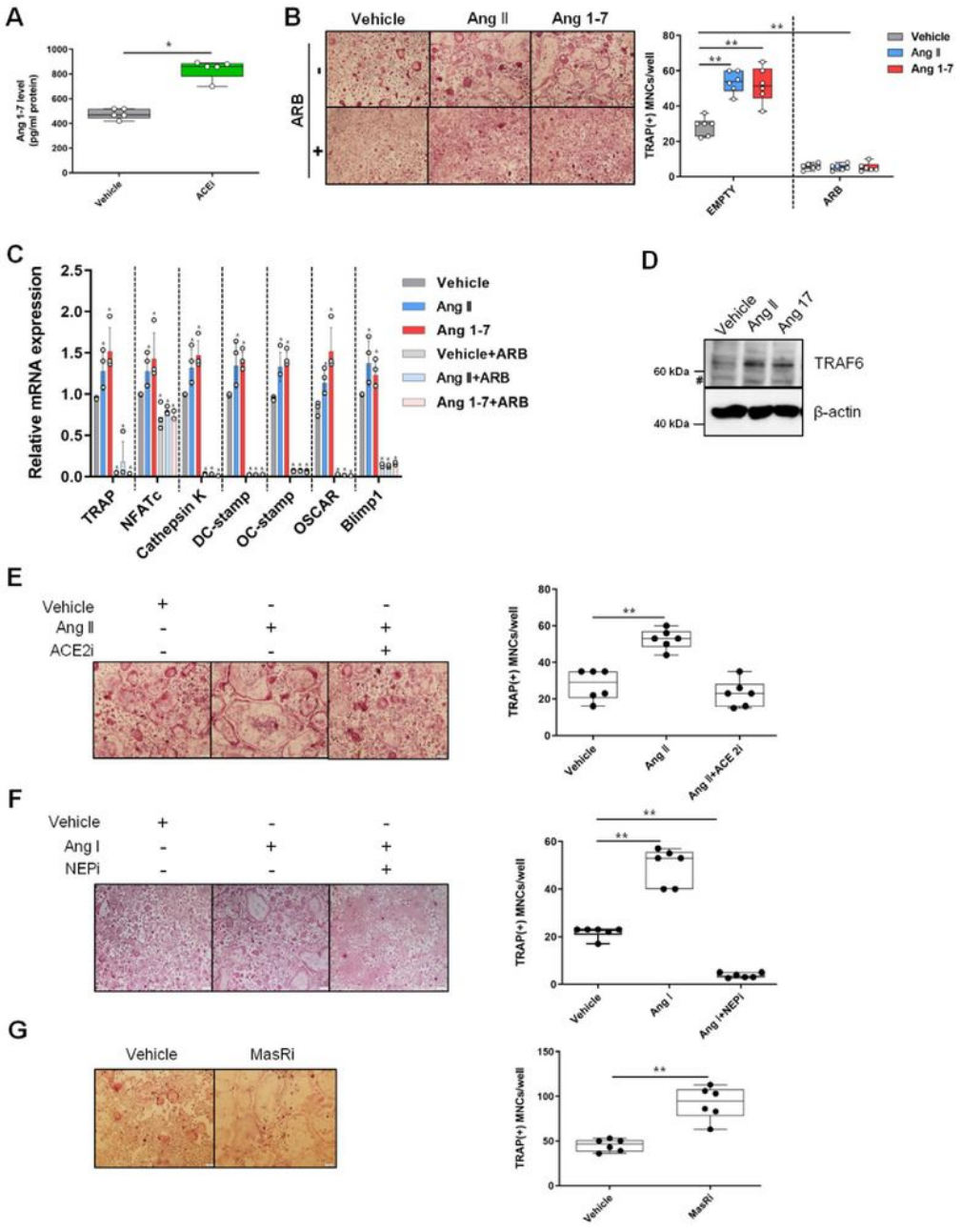

Fig. 4.

Figure 4

Ang 1-7 promoted osteoclast differentiation in mouse cells. (a) Level of Ang 1-7 measured using ELISA in osteoclast culture media with/without ACEi (1×10^{-5} M captopril). (b-c) Mouse bone marrow monocytes were treated with Ang II (1×10^{-6} M) or Ang 1-7 (1×10^{-6} M) with/without ARB (1×10^{-5} M losartan). (b) Representative TRAP staining images (left) and the number of TRAP-positive MNCs (>3 nuclei) per well (right). (c) RT-qPCR analysis. (d) Western blotting analysis of Ang II- or Ang 1-7-treated RAW 264.7 cells.

Hash indicates nonspecific bands. (e-g) Representative TRAP staining images (left) and the number of TRAP-positive MNCs (>3 nuclei) per well (right) before and after Ang II (1×10^{-6} M) administration with/without ACE2i (1×10^{-5} M MLN-4760) (e), Ang I (1×10^{-6} M) with/without NEPi (1×10^{-5} M sacubitrilat) (f), and Ang I with/without MasRi (1×10^{-5} M A779) (g). Scale bar = 50 μm. ACE2i, angiotensin-converting enzyme 2 inhibitor; Ang, angiotensin; MasRi, Mas receptor inhibitor; MNCs, multi-nuclear cells; NEPi, neprilysin inhibitor; TRAP, tartrate-resistant acid phosphatase. Values are presented as mean ± SD.; *$p < 0.05$, **$p < 0.01$ using Mann-Whitney U test.

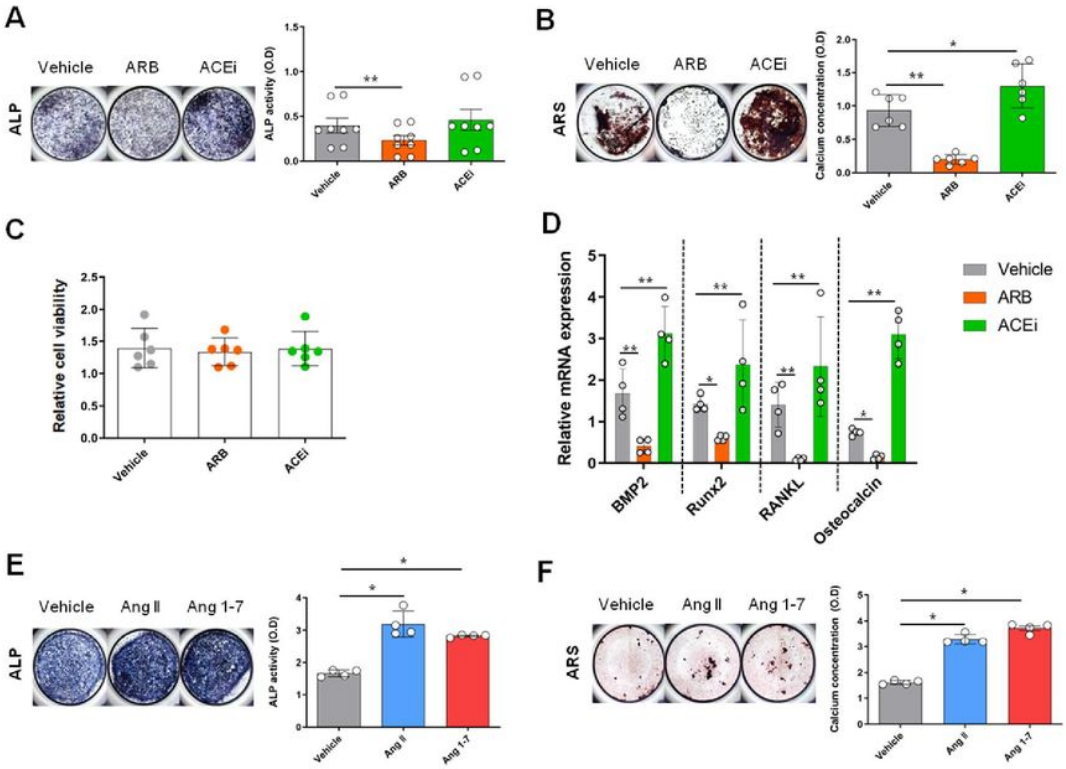

Fig. 5.

Figure 5

ARB, but not ACEi, inhibited osteoblast differentiation in mouse cells. (a-d) ARB (1×10^{-5} M losartan) or ACEi (1×10^{-5} M captopril) administered to primary mouse osteoblastic cells. (a) ALP staining (left) and ALP activity (right). (b) ARS staining (left) and its quantification (right). (c) CCK-8 assay (d) RT-qPCR analysis. (e-f) Ang II (1×10^{-6} M) or Ang 1-7 (1×10^{-6} M) applied to primary mouse osteoblastic cells. (e) ALP staining (left) and ALP activity (right). (f) ARS staining (left) and its quantification (right). ACEi, angiotensin-converting enzyme inhibitor; ALP, alkaline phosphatase; Ang, angiotensin; ARB, angiotensin II

receptor blocker; ARS, alizarin red. Values are presented as mean ± SD.; *$p < 0.05$, **$p < 0.01$ using Mann-Whitney *U* test.

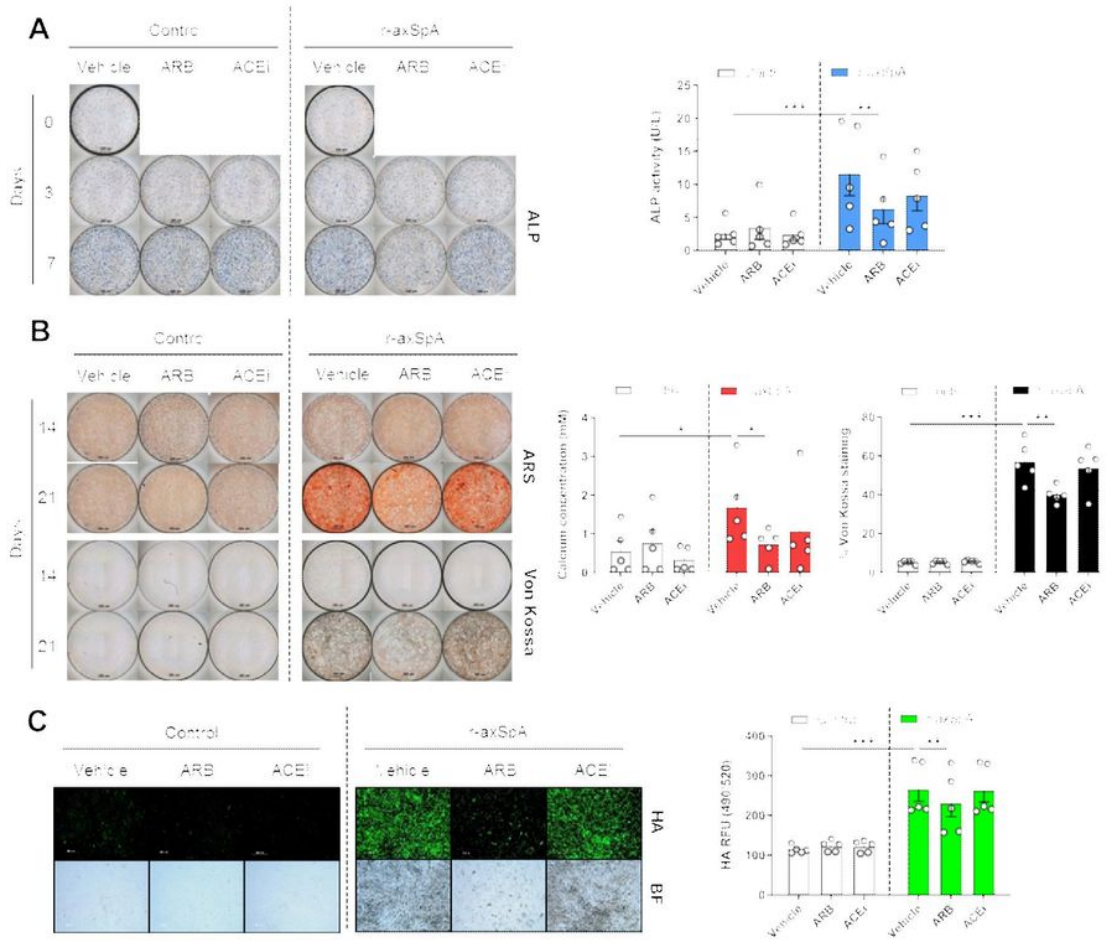

Fig. 6.

Figure 6

ARB suppressed osteoblast differentiation from BdCs of r-axSpA patients. (a-c) BdCs of control and r-axSpA patients were differentiated into osteoblasts using ARB (1×10^{-5} M losartan) or ACEi (1×10^{-5} M captopril). (a) ALP staining (left) and ALP activity (right). (b) ARS and Von Kossa staining (left) and its quantification (right). (c) HA staining (left) and quantification (right). Scale bar = 200 μm. ACEi, angiotensin-converting enzyme inhibitor; ALP, alkaline phosphatase; Ang, angiotensin; ARB, angiotensin II receptor blocker; ARS, alizarin red; AT1R, angiotensin II type 1 receptor; BdCs, bone-derived cells; HA,

hydroxyapatite. Values are presented as mean ± SD.; *$p < 0.05$, **$p < 0.01$, ***$p < 0.001$ using Mann-Whitney *U* test.

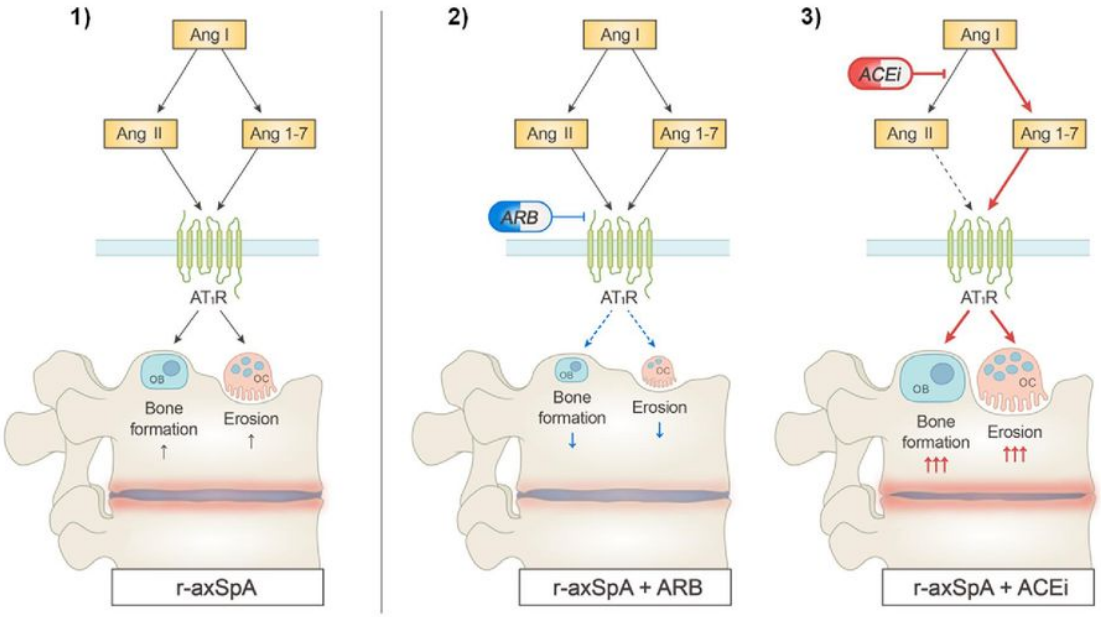

Fig. 7.

Figure 7

Schematic model showing the role of RAS inhibitors in SpA-associated bone changes. 1) Osteoclast and osteoblast differentiation increased in r-axSpA possibly because of the increase in the expression of RAS molecules, culminating in aberrant bone formation and erosion. 2) ARB inhibited binding of Ang II and Ang 1-7 to AT1R, resulting in suppression of osteoclast and osteoblast differentiation. 3) ACEi inhibited conversion of Ang I into Ang II and augmented production of Ang 1-7, leading to increased osteoblast and osteoclast differentiation, which caused higher bone formation and erosion. Ang, angiotensin; ACEi, angiotensin-converting enzyme inhibitor; ARB, angiotensin II receptor blocker; AT1R, angiotensin II type 1 receptor; RAS, renin-angiotensin system; r-axSpA, radiographic axial spondyloarthritis.

Supplementary Files

This is a list of supplementary files associated with this preprint. Click to download.

- Supplementaryfigures.docx